Published in final edited form as:
Tetrahedron. 2007 April 16; 63(16): 3287–3292.

A unique quinolineboronic acid-based supramolecular structure that relies on double intermolecular B-N bonds for self-assembly in solid state and in solution

Yanling Zhang[a], **Minyong Li**[a], **Sekar Chandrasekaran**[a], **Xingming Gao**[a], **Xikui Fang**[b], **Hsiau-Wei Lee**[a], **Kenneth Hardcastle**[b], **Jenny Yang**[a], and **Binghe Wang**[a,*]

a*Department of Chemistry and Center for Biotechnology and Drug Design, Georgia State University, Atlanta, GA 30302-4089*

b*X-ray Crystallography Center, Department of Chemistry, Emory University, Atlanta, GA 30322*

Abstract

The boronic acid functional group plays very important roles in sugar recognition, catalysis, organic synthesis, and supramolecular assembly. Therefore, understanding the unique properties of this functional group is very important. 8-Quinolineboronic acid (8-QBA) is found to be capable of self-assembling in solid state through a unique intermolecular B-N bond mechanism reinforced by intermolecular boronic anhydride formation, π-π stacking, and hydrogen bond formation. NMR NOE and diffusion studies indicate that intermolecular B-N interaction also exists in solution with 8-QBA. In contrast, a positional isomer of 8-QBA, 5-quinolineboronic acid (5-QBA) showed very different behaviors in crystal packing and in solution and therefore different supramolecular network. Understanding the structural features of this unique 8-QBA assembly could be very helpful for the future design of new sugar sensors, molecular catalysts, and supramolecular assemblies.

Keywords

Quino lineboronic acid; Self-assembly; Crystal structure; NMR

1. Introduction

Boron compounds are very useful in a wide variety of ways in organic, bioorganic, and medicinal chemistry. For example, because of its open shell, boron-based compounds have been widely used as Lewis acids for chelation and catalysis applications.[1-3] Boronic acids are known to bind the diol moiety and thus have been widely used in the field of sensing and sugar recognition.[4-14] In addition, there is a strong interest in the synthesis of new boronic acids as potential boron neutron capture therapy (BNCT) agents,[15-17] antiviral agents,[18,19] and enzyme inhibitors.[20-24,19,25-29] Recently, boronic acids have been used as promising building blocks in crystal engineering, in which various types of novel supramolecular assemblies have been generated.[30-35] For example, Strongin and co-workers found that a tetraarylboronic acid resorcinarene could form an infinite two-dimensional array through extensive hydrogen bond interactions.[30] Wuest and Galoppini recently reported a new

* Corresponding author. Tel.: +1-404-651-0289; fax: +1-404-654-5827; email: wang@gsu.edu..

molecular tectonics with 3-D supramolecular channel networks using the $–B(OH)_2$ moiety of tetraboronic acid.[31] The Hopfl and Pedireddi labs generated different types of hydrogen-bonding supramolecular assemblies systems utilizing phenylboronic acid and its derivatives.[32,33] Lavigne and colleagues reported self-repairing polymers[36,37] based on boronic acid-diol interactions.[8,38,27] Jäkle and co-workers also developed boron-containing polyolefins as Lewis acid catalysts and precursor to luminescent materials, sensors and other materials.[39-41]

We envision that the boronic acid functional group can also be used to build supramolecular architectures by taking advantage of its unique and strong Lewis acidity. Therefore, a boronic acid compound with an appropriately positioned Lewis base should allow for tight self-assembly of the boronic acid compound.[35,42] Herein we report one such example in which 8-quinolineboronic acid (8-QBA) is shown to self-assemble into a dimer in solid state as determined by X-ray crystallography. NMR studies also indicate the same tendency to self-assembly in solution.

2. Results and Discussion

Again, we are interested in taking advantage of the unique Lewis acidity of the boron due to its open shell for constructing unique boronic acid-based self-assembly systems. In doing so, one can envision an approach that uses B-N bond formation as a way to achieve self-recognition. B-N bond formation involving a boronic acid in an intramolecular fashion has been reported, especially in crystalline states and in aprotic solvents.[43-53,35] For example, Wulff and colleagues reported reversible formation of a B-N bond when an amine is in a 1,5-relationship with a boronic acid.[43] A boronic acid protease inhibitor was found to have intramolecular B-N bond formation when the boron atom and an amine group is in a 1-6 relationship.[46] Livant reported B-N bond formation involving trapped boric acid which is positioned closely to an amino group.[44] In all these examples, strong intramolecular B-N interactions only occur under favorable entropic conditions. Therefore, for B-N mediated self-assembly to work there needs to have a secondary reinforcement for the interaction to be strong enough. Another relevant system worth mentioning is an anthracene-based fluorescent boronic acid reported by the Shinkai lab, which changes fluorescent properties upon sugar binding.[54,55] Initially, it was thought that strong B-N bond formation was the reason for the increased fluorescent intensity upon sugar binding. Our lab has recently shown that solvolysis is responsible for the observed fluorescent intensity changes.[52,56] Such a mechanism is further substantiated by crystal structural studies of the Anslyn lab.[42]

Upon a close examination of the structure of 8-QBA (Figure 1), it appears that the relative orientation and positions of the quinoline nitrogen and the boronic acid moiety are perfect for bidentate self-assembly. Hence, we were very interested in studying the supramolecular properties of 8-QBA to see whether self-association happens or not. As a comparison, we were also interested in studying 5-QBA.

The crystals of 8-QBA and 5-QBA were obtained from methanol solution and their structures were determined by X-ray diffraction. Indeed, 8-QBA self-assembles through the formation of two complementary B-N bonds leading to the formation of a dimer (Figure 2). The B-N interactions are reinforced by the formation a boronic anhydride group resulting from the loss of one water molecule. [57] To the best of our knowledge, this is the first example where a boronic acid supramolecular structure is based on this kind of double B-N interactions. The shape of the dimer resembles that of a chair with an angle of 104.7 °, which is consistent with the sp^3 hybridization state of the boron atoms at the hinge position. This dimeric structure is in direct contrast to that of 5-QBA (Figure 3), which exists in a monomeric form.[58] It seems that the ability for 8-QBA to form two B-N bonds is the main reason that differentiates these

two and allows for dimer formation in 8-QBA. The further ordering of the dimeric units of 8-QBA is dependent on π-stacking of the quinoline rings and hydrogen bond formation between the boronic anhydride units (Figures 4 and 5). There are two hydrogen bonds between two neighboring boronic anhydride units, which are reinforced by the presence of four additional hydrogen bonds involving two water molecules (Figure 4). The hydrogen bond distances range from 1.67 to 1.91 Å, indicating strong interactions. There also exist strong π-π stacking in the supramolecular structure. In each dimeric unit (Figure 5), one quinoline ring shows π-π overlap with two adjacent aromatic rings and the other shows stacking with only one. In a face to face stacking, the distance between two aromatic rings is 3.6 Å (Figure 4), which approaches the van der Waals minimally allowable radius, again indicating strong interactions.

As a comparison, the crystal structure of 5-QBA (Figure 3) has also been examined. The pattern of recognition and self-assembly between two 5-QBA units (Figure 6) is understandably different from that of 8-QBA. First, B-N bond formation does not play any role in the intermolecular interactions in 5-QBA. Instead, the assembly is controlled by head to head hydrogen bond formation between boronic acid units. There is one water molecule bridging between the quinoline nitrogen and a boronic acid hydroxyl group on a neighboring molecule. As consequence, each water molecule is engaged in three hydrogen bonds, one through its oxygen and two through its two hydrogen atoms. Similarly, each hydroxyl group of the boronic acid moiety is engaged in two hydrogen bond interactions, one through its hydrogen and one through its oxygen. This intricate hydrogen bond network seems to be the dominant force in crystal packing. Second, the boron atom is in the sp^2 hybridized form, giving it a planary shape. However, the boron atom is twisted out of the plane of the aromatic system allowing hydrogen bond formation in a “vertical” fashion and π–π-stacking between the aromatic systems.

$$THC_{\text{Donor}-\text{accept}}[\%] = THC_{DA}[\%] = \left[1 - \frac{\sum_{n=1-6} |\,109.5 - \theta_n\,|^{\circ}}{90^{\circ}}\right] \times 100 \qquad \text{(Equation 3)}$$

With B-N bond formation in 8-QBA, the boron atom exists in the tetrahedral form. The tetrahedral character THC_{DA}[%] of the two boron atoms in 8-QBA structure have been calculated from a formula introduced by Höpfl, that includes all six bond angles around the boron atom(Equation 3). For the B1 atom, the d (N1→B1) bond length is 1.708 (3) Å and the tetrahedral character THC_{DA}[%] is 77.53. For B2 atom, the d(N2→B2) bond length is 1.693 (3) Å and the tetrahedral character THC_{DA}[%] is 80.58. The results agree with those listed by Höpfl and Norrild for related compounds.[32,49,45] 5-QBA on the other hand has no N-B interaction and exists in the trigonal form.

Although the crystal structure clearly shows intermolecular B-N bond formation in 8-QBA, it was not clear whether in solution such interactions would be strong enough to promote dimer formation. In order to probe this issue, we have used NMR to examine the NOE effect. Therefore, 2-D NOESY experiments were conducted (Figure 7 and 8). If 8-QBA exists in a dimer form in solution, we would expect to see NOE effect between H_A and H_D (Figure 7). Indeed, the NOESY spectrum at 115 mM in deuterated methanol shows an intense cross peak (H_A/H_D) corresponding to the interaction between H_A proton of one 8-QBA and H_D proton of the other 8-QBA unit (Figure 8). This could only arise from dimer formation since the intermolecular distance between H_A and H_D in a non-associated form would be too long to allow for the observed NOE.

Furthermore, there was no NOE observed between H_E and H_F, which has the same relationship as H_A and H_D if there was no dimer formation. Using the X-ray H_A-H_F distance of 2.30 Å as reference, the calculated H_A-H_D distance determined by NOESY in solution is 2.71 Å, which is close to that obtained from X-ray crystallographic studies (2.98 Å). The

results suggest that 8-QBA exist as a dimer in methanol solution under the conditions of the experiments. In contrast, 5-QBA showed no such intermolecular NOE effect.

In addition to the NOE experiments, we were also interested in studying the molecular radius of 8-QBA at different concentrations. We envisioned that if self-association happens, one would expect to see increased apparent molecular radius. The pulsed field gradient (PFG) NMR techniques have long been used for the direct measurement of diffusion coefficients,[59] which can be converted to molecular radii. [60] Therefore, 8-QBA was dissolved in methanol-d_6 at 1.0, 25, 50, 115 mM concentrations with dioxane spiked in as an internal reference (about 100 mM). [61] The diffusion constants were obtained via fitting the integrated area of the resonance of each arrayed spectrum into the Stejskal-Tanner equation.[62] The same experiments were conducted with 5-QBA as a comparison.

Table 1 summarizes the results of the molecular diffusion experiments. At 115 mM, the molecular radius of 8-QBA (5.43 Å) is 20% greater than that of 5-QBA (4.50 Å) at the same concentration. The molecular radius of 8-QBA also increases by 20% when its concentration changes from 1 mM to 115 mM. It needs to be noted that since 8-QBA is not a spherical molecule, one would not expect the dimer to have a molecular radius twice that of the monomer. Furthermore, self association in solution is not an “all or none” situation. It is a concentration dependent event with the fraction of those in the dimer form related to the association constant and 8-QBA concentration. Thus the molecular radii determined are the average results of the monomer and dimer forms and are depending on the fraction of 8-QBA in the dimer form and the true molecular radius of the dimer. The combined results of the NOE and diffusion studies indicate that in solution 8-QBA exists in the dimer form in sufficient quantity at 115 mM to give rise to a strong NOE effect between H_A and H_D and to show an increased apparent molecular size. All indications are that self-association of 8-QBA does occur in solution (methanol) as well.

3. Conclusion

In conclusion, we have demonstrated that 8-quinoline boronic acid (8-QBA) forms a dimer through the formation of two B-N bonds reinforced by intermolecular anhydride formation, hydrogen bonds, and π–π-stacking in crystal form. NMR studies indicate that the same dimer form exists in solution as well. Such results may help the future design of boronic acid-based new molecules, supramolecular assemblies, and materials for organic, bioorganic, medicinal and crystal engineering applications.

4. Experimental

Chemicals and solvents were obtained from Frontier Scientific, Aldrich, and Acros and used without purification. Crystals were grown from a mixture of methanol and methylene chloride.

4.1 X-ray crystallographic studies

Suitable crystals each of 5-QBA and 8-QBA were coated with Paratone-N oil, suspended in small fiber loops and placed in a cooled nitrogen gas stream at 173 K on a Bruker D8 SMART 1000 CCD sealed tube diffractometer using CuK_α radiation. Data were measured using a series of combinations of phi and omega scans with 10 s frame exposures and 0.3° frame widths. Data collection, indexing and initial cell refinements were all carried out using SMART [63] software. Frame integration and final cell refinements were done using SAINT software.[64] The SADABS[65] program was used to carry out absorption corrections.

The structures were solved using Direct methods and difference Fourier techniques (SHELXTL, V6.12).[66] All the hydrogen atoms were located in a difference Fourier map and

were included in the final cycles of least squares with isotropic U_{ij}'s or as riding atoms; all non-hydrogen atoms were refined anisotropically. Scattering factors and anomalous dispersion corrections are taken from the *International Tables for X-ray Crystallography*.[67] Structure solution, refinement, graphics and generation of publication materials were performed by using SHELXTL, V6.12 software. Additional details of data collection and structure refinement are given in Table 1 of the Supplemental Materials section.

4.2 NMR studies

The NOE studies were conducted in deuterated methanol at 115 mM. Pulsed field gradient (PFG) NMR techniques were used for the direct measurement of diffusion coefficients.[59] 8-QBA and 5-quinolineboronic acid (5-QBA) were dissolved in methanol-d_4 at 1.0, 25, 50, 115 mM respectively. The spectra were collected using a modified PG-SLED pulse sequence with 16 or 8 K complex data points for each FID with dioxane spiked in as an internal reference (about 100 mM) at 25 °C.[61] The diffusion constants were obtained via fitting the integrated area of the resonance of each arrayed spectrum into the Stejskal-Tanner equation (Equation 1).[62]

$$A = A_0 \exp \qquad \text{(Equation 1)}$$

Where γ is the gyromagnetic ratio of proton (26752), δ is the PFG duration time (2 ms), and Δ is the time between PFG pulses (200 ms). The gradient strength (*G*) was arrayed from 0.195 G/cm to 28.32 G/cm using 25 steps. *A* is the integrated area of desired resonances at each array spectrum after subtraction of baselines. A_0 is the integrated area of the desired resonances when the PFG strength is minimal.[68] The data are treated by plotting the log of the signal intensity against $(\gamma\delta G)^2$ (Δ - δ/3), the slope of which gives the diffusion coefficient.

The diffusion coefficient (*D*) is related to the size of the diffusing object according to the Einstein-Stokes equation (Equation 2). [60]

$$D = KT / 6\pi\eta R_H \qquad \text{(Equation 2)}$$

where *K* is Boltzmann constant (1.38×10^{-23} J/K), η is viscosity of methanol-d_4 at 25 °C (5.2×10^{-4} Pa·s), and *T* is absolute temperature (298 K).

Supplementary Material

Refer to Web version on PubMed Central for supplementary material.

Acknowledgements

Financial support from the National Institutes of Health (CA123329**,** CA88343, CA113917, NO1-CO-27184), the Georgia Cancer Coalition through a Distinguished Cancer Scientist Award, and the Georgia Research Alliance through an Eminent Scholar endowment and Eminent Scholar Challenge grants is gratefully acknowledged.

References

1. Roy CD. Aust J Chem 2006;59:657–659.
2. Cho, BT. In Boronic Acids. Hall, DG., editor. Wiley-VCH; Weinheim : 2005. p. 411-439.
3. Ishihara, K. In Boronic Acids. Hall, DG., editor. Wiley-VCH; Weinheim : 2005. p. 101-121.
4. Wang W, Gao X, Wang B. Curr Org Chem 2002;6:1285–1317.
5. Cao HS, Heagy MD. J Fluoresc 2004;14:569–584. [PubMed: 15617264]
6. Hall, DG., editor. Boronic Acids: Preparation and Applications in Organic Synthesis and Medicine. Wiley-VCH; 2005.
7. Lorand JP, Edwards JO. J Org Chem 1959;24:769–774.

8. Springsteen G, Wang B. Tetrahedron 2002;58:5291–5300.
9. Wiskur SL, Lavigne JJ, Metzger A, Tobey SL, Lynch V, Anslyn EV. Chem-A Eur J 2004;10:3792–3804.
10. James TD, Linnane P, Shinkai S. Chem Commun 1996:281–288.
11. Ward CJ, Patel P, James TD. Org Lett 2002;4:477–479. [PubMed: 11843570]
12. Alexeev VL, Sharma AC, Goponenko AV, Das S, Lednev IK, Wilcox CS, Finegold DN, Asher SA. Anal Chem 2004;75:2316–2323. [PubMed: 12918972]
13. Shinkai S, Takeuchi M. Trend Anal Chem 1996;15:188–193.
14. Jiang S, Rusin O, Escobedo JO, Kim KK, Yang Y, Fakode S, Warner IM, Strongin RM. J Am Chem Soc 2006;128:12221–12228. [PubMed: 16967973]
15. Soloway AH, Tjarks W, Barnum BA, Rong FG, Barth RF, Codogni IM, Wilson JG. Chem Rev 1998;98:1515–1562. [PubMed: 11848941]
16. Hawthorne, MF., editor. Angew Chem Int. 32. 1993. p. 950-984.
17. Kabalka GW. Expert Opin Ther Pat 1998;8:545–551.
18. Chen X, Bastow K, Goz B, Kucera L, Morris-Natschke SL, Ishaq KS. Antivir Chem Chemother 1996;7:108–114.
19. Bacha U, Barrila J, Velazquez-Campoy A, Leavitt SA, Freire E. Biochemistry 2004;43:4906–4912. [PubMed: 15109248]
20. Suenaga H, Yamamoto H, Shinkai S. Pure Appl Chem 1996;68:2179–2186.
21. Adams J, Behnke M, Chen SW, Cruickshank AA, Dick LR, Grenier L, Klunder JM, Ma YT, Plamondon L, Stein RL. Bioorg Med Chem Lett 1998;8:333–338. [PubMed: 9871680]
22. Lebarbier C, Carreaux F, Carboni B, Boucher JL. Bioorg Med Chem Lett 1998;8:2573–2576. [PubMed: 9873583]
23. Teicher BA, Ara G, Herbst R, Palombella VJ, Adams J. Clin Cancer Res 1999;5:2638–2645. [PubMed: 10499643]
24. Adams J, Kauffman M. Can Invest 2004;22:304–311.
25. Johnson LL, Houston TA. Tetrahedron Lett 2002;43:8905–8908.
26. Myung J, Kim KB, Crews CM. Med Res Rev 2001;21:245–273. [PubMed: 11410931]
27. Yan J, Fang H, Wang B. Med Res Rev 2005;25:490–520. [PubMed: 16025498]
28. Yang, W.; Gao, S.; Wang, B. In Organoboronic Acids. Hall, D., editor. John Wiley and Sons; New York: 2005. p. 481-512.
29. Yang W, Gao X, Wang B. Med Res Rev 2003;23:346–368. [PubMed: 12647314]
30. Lewis PT, Davis CJ, Fronczek FR, Strongin RM. Org Lett 2001;3:2443–2445. [PubMed: 11483030]
31. Fournier JH, Maris T, Wuest JD, Guo WZ, Galoppini E. J Am Chem Soc 2003;125:1002–1006. [PubMed: 12537499]
32. Höpfl H. J Organomet Chem 1999;581:129–149.
33. Pedireddi VR, Lekshmi NS. Terrahedron Lett 2004;45:1903–1906.
34. Rodriguez-Cuamatzi P, Arillo-Flores OI, Bernal-Uruchurtu MI, Höpfl H. Cryst Growth Des 2005;5:167–175.
35. Barba V, Hápfl H, Farfán N, Santillan R, Beltran HI, Zamudio-Rivera LS. Chem Commun 2004:2834 – 2835.
36. Niu WJ, Rambo B, Smith MD, Lavigne JJ. Chem Commun 2005;41:5166–5168.
37. Niu WJ, O'Sullivan C, Rambo BM, Smith MD, Lavigne JJ. Chem Commun 2005;34:4342–4344.
38. Yan J, Springsteen G, Deeter S, Wang B. Tetrahedron 2004;60:11205–11209.
39. Qin Y, Cheng G, Sundararaman A, Jäkle F. J Am Chem Soc 2002;124:12672–3. [PubMed: 12392409]
40. Jäkle F. J Inorg Organomet Polym Mater 2005;15:293–307.
41. Qin Y, Pagba C, Piotrowiak P, Jäkle F. J Am Chem Soc 2004;126:7015–8. [PubMed: 15174871]
42. Zhu L, Shabbir SH, Gray M, Lynch VM, Sorey S, Anslyn EV. J Am Chem Soc 2006;128:1222–1223. [PubMed: 16433539]
43. Burgemeister T, Grobe-Einsler R, Grotstollen R, Mannschreck A, Wulff G. Chem Ber 1981;114:3403–3411.

44. Livant PD, Northcott DJD, Shen YP, Webb TR. J Org Chem 2004;69:6564–6571. [PubMed: 15387578]
45. Norrild JC, Sotofte I. J Chem Soc Perkin Trans 2001;2:727–732.
46. Snow RJ, Bachovchin WW, Barton RW, Campbell SJ, Coutts SJ, Freeman DM, Gutheil WG, Kelly TA, Kennedy CA, Krolikowski DA, Leonard SF, Pargellis CA, Tong I, Adams J. J Am Chem Soc 1994;116:10860–10869.
47. Sudmeier JL, Gunther UL, Gutheil WG, Coutts SJ, Snow RJ, Barton RW, Bachovchin WW. Biochemistry 1994;33:12427–12438. [PubMed: 7918465]
48. Toyota S, Futawaka T, Asakura M, Ikeda H, Oki M. Organometallics 1998;17:4155–4163.
49. Norrild JC. J Chem Soc Perkin Trans 2001;2:719–726.
50. Fjeldberg T, Gundersen G, Jonvik T, Seip HM, Saeboe S. Acta Chem Scand Series A: Phys Inorg Chem 1980;34:547–565.
51. Ostby KA, Gundersen G, Haaland A, Noth H. Dalton Transaction 2005;13:2284–2291.
52. Franzen S, Ni W, Wang B. J Phys Chem B 2003;107:12942–12948.
53. Ni W, Kaur G, Springsteen G, Wang B, Franzen S. Bioorg Chem 2004;32:571–81. [PubMed: 15530997]
54. Sandanayake KRAS, Shinkai S. J Chem Soc Chem Commun 1994:1083–1084.
55. James TD, Sandanayake KRAS, Shinkai S. Chem Commun 1994:477–478.
56. Ni W, Kaur G, Springsteen G, Wang B, Franzen S. Bioorg Chem 2004;32:571–81. [PubMed: 15530997]
57. *Crystal data for 8-QBA:* , ($C_{18}H_{16}B_2N_2O_4$), M = 345.95, Monoclinic, P2(1)/c; 0.33 × 0.22 × 0.17 mm, a = 8.3643(3), b = 17.5044(5), c = 11.0456(3) Å,α = 90, β= 91.511(2), γ = 90°, V= 1616.65(9) $Å^3$, *Z*= 4, *D* = 1.421 g/cm3, μ = 0.810 mm-1,8341 total reflections, *R*1 = 0.0508 and w*R*2 = 0.1448. CDDC 635581.
58. *Crystal data for 5-QBA:* , ($C_9H_{10}BNO_3$), M = 190.99, Monoclinic, C2/c; 0.35 × 0.33 × 0.31mm, a =17.5355(10), b = 7.1309(4), c = 15.2705(9) Å, α=90, β= 93.576(3), γ= 90°, V=1905.76(19) Å3, Z= 8, D = 1.331 g/cm3, μ = 0.815 mm-1, 44121905.76(19) total reflections, *R*1 = 0.0467 and w*R2* = 0.1259. CDDC 635580.
59. Altieri AS, Hinton DP, Byrd RA. J Am Chem Soc 1995;117:7566–7567.
60. Kholodenko AL, Douglas JF. Phys Rev E 1995;51:1081–1090.
61. Martichonok K, Jones JB. Bioorg Med Chem 1997;5:679–684. [PubMed: 9158866]
62. Stejskal EO, Tanner JE. J Chem Phys 1965;42:288–292.
63. SMART Version 5.625. Bruker AXS, Inc., Analytical X-ray Systems: 5465 East Cheryl Parkway, Madison WI 53711-5373, 2002
64. SAINT Version 6.36A. Bruker AXS, Inc., Analytical X-ray Systems 5465 East Cheryl Parkway, Madison WI 53711-5373, 2002
65. Sheldrick G, SADABS V2.10. University of Göttingen, 2003
66. SHELXTL V6.12. Bruker AXS, Inc., Analytical X-ray Systems 5465 East Cheryl Parkway, Madison WI 53711-5373, 2002
67. Wilson, AJC. Ed International Tables for X-ray Crystallography. C. Academic Publishers; Dordrecht: 1992.
68. Lee HW, Yang W, Ye Y, Liu ZR, Glushka J, Yang JJ. Biochim Biophys Acta 2002;1598:80–87. [PubMed: 12147347]

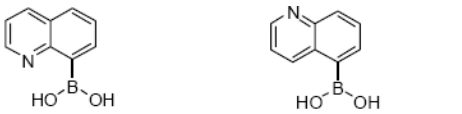

8-Quinilineboronic acid (8-QBA) 5-Quinilineboronic acid (5-QBA)

Figure 1.
The structures of 8-QBA and 5-QBA

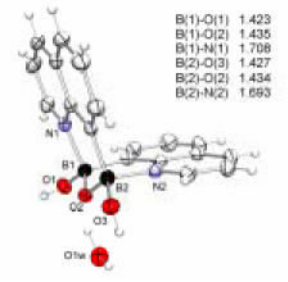

Figure 2.
Crystal structure of 8-QBA dimer with thermal ellipsoids shown at 50% probability level

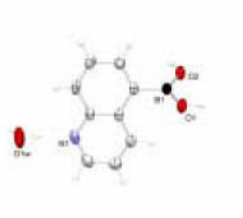

Figure 3.
Crystal structure of 5-QBA with thermal ellipsoids shown at 50% probability level

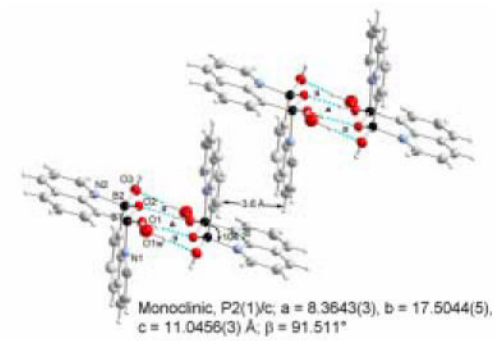

Figure 4.
Perspective view of the molecular recognition pattern of 8-QBA: a hydrogen bondeddimer of $H_2(B_2O_3)(C_9NH_6)\cdot H_2O$.

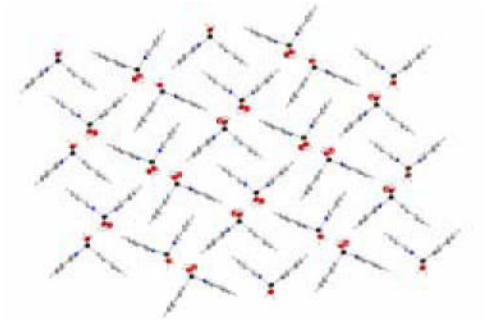

Figure 5.
3-D supramolecular network of 8-QBA through π-π interactions and hydrogen bonds

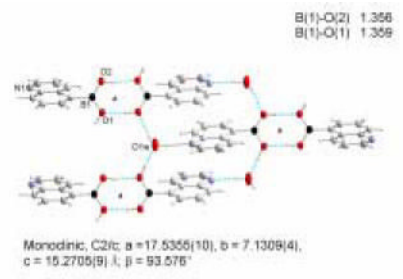

Figure 6.
A cyclic hydrogen bond network is the dominant force in crystal packing for 5-QBA.

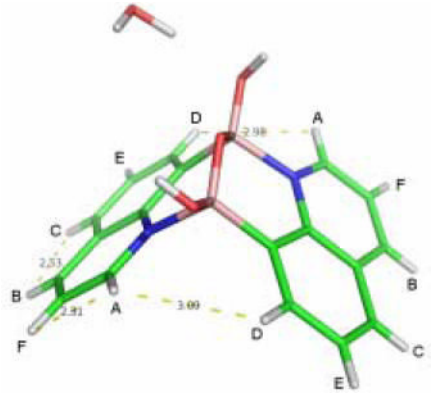

Figure 7.
The structure of 8-QBA dimer

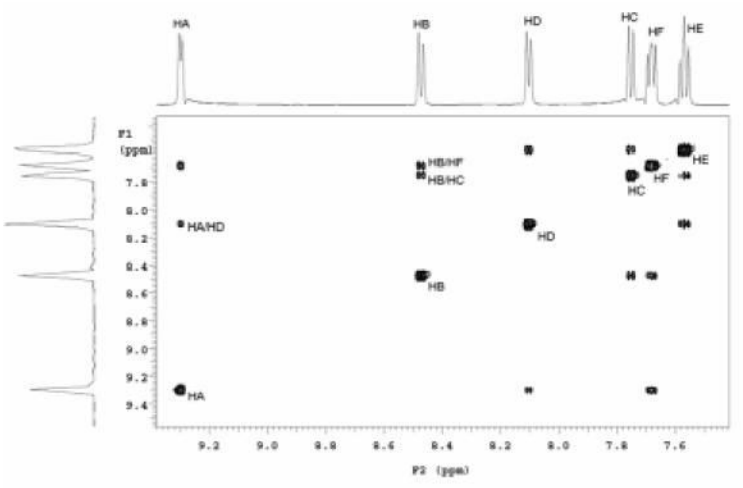

Figure 8.
2D-NOESY spectrum of 8-QBA measured in CD_3OD

Table 1

The results of molecular diffusion experiments for 8-QBA and 5-QBA.

Concentration	5-QBA Studies				8-QBA Studies			
	5-QBA		Internal dioxane reference		8-QBA		Inter	
	Diffusion Constant ($\times 10^{-6}$ cm^2/s)	Molecular Radius (Å)	Diffusion Constant ($\times 10^{-6}$ cm^2/s)	Molecular Radius (Å)	Diffusion Constant ($\times 10^{-6}$ cm^2/s)	Molecular Radius (Å)	Diffusion Constant ($\times 10^{-6}$ cm^2/s)	
1 mM	10.6	3.96	18.5	2.27	9.32	4.50	19.4	
25 mM	10.6 ±0.2	3.95±0.08	16.7 ±0.06	2.53±0.01	8.08 ±0.13	5.20±0.08	18.9 ±2.6	
50 mM	11.3 ±0.2	3.72±0.07	16.8 ±0.15	2.49±0.02	7.87 ±0.04	5.33±0.03	17.0 ±0.2	
115 mM	9.32 ±0.06	4.50±0.03	15.9 ±0.6	2.65±0.10	7.74 ±0.34	5.43±0.24	16.6 ±0.1	